# Long-term characterization of roadside air pollutants in urban Beijing and associated public health implications

Wu, Xuefang; Vu, Tuan V.; Harrison, Roy M.; Yan, Jing; Hu, Xiaohan; Cui, Yangyang; Shi, Aijun; Liu, Xinyu; Shen, Yan; Zhang, Gen; Xue, Yifeng

*DOI:*
10.1016/j.envres.2022.113277

# Long-term Characterization of Roadside Air Pollutants in Urban Beijing and Associated Public Health Implications

Xuefang Wu[1], Tuan V. Vu[3], Roy M. Harrison[4,5], Jing Yan[1], Xiaohan Hu[6], Yangyang Cui[1], Aijun Shi[7], Xinyu Liu[1], Yan Shen[1], Gen Zhang[2*], Yifeng Xue[1*]

[1]National Engineering Research Center of Urban Environmental Pollution Control, Beijing Municipal Research Institute of Environmental Protection, Beijing 100037, China

[2]State Key Laboratory of Severe Weather and Key Laboratory for Atmospheric Chemistry of the China Meteorological Administration (CMA), Institute of Atmospheric Composition, Chinese Academy of Meteorological Sciences (CAMS), Beijing, 100081, China

[3]School of Public Health, Imperial College London, London, United Kingdom

[4]Division of Environmental Health and Risk Management, School of Geography, Earth and Environmental Sciences, University of Birmingham, Edgbaston, Birmingham B15 2TT, United Kingdom

[5]Department of Environmental Sciences/Centre of Excellence in Environmental Studies, King Abdulaziz University, PO Box 80203, Jeddah, 21589, Saudi Arabia

[6]Beijing Pollution Source Management Affairs Center, Beijing 100089, China

[7]Beijing Vehicle Emission Management Affair Centre, Beijing 102612, China

[*] Corresponding authors. Email: zhanggen@cma.gov.cn (Gen Zhang), xueyifeng@cee.cn (Yifeng Xue)

**Abstract:**

Road traffic constitutes a major source of air pollutants in urban Beijing, which are responsible for substantial premature mortality. A series of policies and regulations has led to appreciable traffic emission reductions in recent decades. To shed light on long-term (2014-2020) roadside air pollution and assess the efficacy of traffic control measures and their effects on public health, this study quantitatively evaluated changes in the concentrations of six key air pollutants ($PM_{2.5}$, $PM_{10}$, $NO_2$, $SO_2$, CO and $O_3$) measured at 5 roadside and 12 urban background monitoring stations in Beijing. We found that the annual mean concentrations of these air pollutants were remarkably reduced by 47% to 71% from 2014 to 2020, while the concurrent ozone concentration increased by 17.4%. In addition, we observed reductions in the roadside increments in $PM_{2.5}$, $NO_2$, $SO_2$ and CO of 54.8%, 29.8%, 20.6%, and 59.1%, respectively, indicating the high effectiveness of new vehicle standard (China V and VI) implementation in Beijing. The premature deaths due to traffic emissions were estimated to be 8379 and 1908 cases in 2014 and 2020, respectively. The impact of $NO_2$ from road traffic relative to $PM_{2.5}$ on premature mortality was comparable to that of traffic-related $PM_{2.5}$ emissions. The public health effect of $SO_2$ originating from traffic was markedly lower than that of $PM_{2.5}$. The results indicated that a reduction in traffic-related $NO_2$ could likely yield the greatest benefits for public health.

**Keywords:** traffic emissions; roadside increment; traffic control policy; $PM_{2.5}$; $NO_2$; health effects

## 1. Introduction

The emissions originating from road traffic are widely acknowledged as a major source of air pollutants in urban areas, and human exposure to air pollutants stemming from road traffic emissions has been demonstrated to generate harmful effects on health (Beelen et al., 2008, Rissler et al., 2012, Pant and Harrison, 2013). Traffic emissions make up a significant fraction of fine particulates ($PM_{2.5}$) in Beijing, accounting for 5-12% of primary $PM_{2.5}$ (Srivastava et al., 2021, Xu et al., 2021), directly emitted by the tailpipes from 2016 to 2017. Road traffic also contributes to secondary particles via gas-to-particle transformation (Pant and Harrison, 2013, Harrison et al., 2021b). In addition, non-exhaust emissions play a significant role in coarse and fine particles, arising from tyre wear, brake wear, and re-suspension of dust, contributing 4-13% to $PM_{2.5}$ in Beijing (Wu et al., 2014, Harrison et al., 2021a, Srivastava et al., 2021). Kam et al. (2012) reported that road vehicular emissions heavily affect small particles, including both primary exhaust particles and secondary species, while the coarse fraction was mostly affected by re-suspension of dust. Additionally, motor vehicles release a very large amount of gaseous pollutants into the atmosphere in Beijing (Cai et al., 2017). According to the Multi-resolution Emission Inventory for China (MEIC, 2018), the transportation sector emitted approximately 6 kt $a^{-1}$, 97 kt $a^{-1}$ and 566 kt $a^{-1}$ of $SO_2$, $NO_x$ and CO, respectively, from 2013 to 2017, accounting for 13%, 40%, 37% of their total primary emissions, respectively. Moreover, a large amount of volatile organic compounds (VOCs) released from vehicle exhaust emissions could contribute to the formation of secondary organic aerosols and ozone, thus enhancing severe haze events in winter (Huang et al., 2014, Li et al., 2017, Harrison et al., 2021a).

To better understand the impact of air pollutants originating from vehicles upon the atmospheric environment and associated health effects, it is important to evaluate the contribution of road traffic emissions and to compare the air quality at different observation sites. Numerous studies have reported the adoption of paired-site data to estimate the contribution from traffic emissions to air pollutants, for example, Harrison and Beddows, (2017) and Wang et al., (2010) estimated the increment due to traffic emissions by subtracting the concentration of air pollutants at urban background monitoring sites from that at proximate roadside sites. For instance, Harrison et al. (2021b) reported that the $PM_{2.5}$ roadside traffic increment reached approximately 5 μg $m^{-3}$ in Beijing during 2016 to 2018, which is similar to that in Paris and Hong Kong. Chen et al. (2018) collected hourly air pollutant data at four traffic stations in

Beijing during 2014 to 2017 and concluded that roadside environments with heavy traffic are highly polluted and should be improved. The characteristics of short-term roadside air pollutants were reported by Zhang et al. (2019b) but just focused on one selected road in fall and winter. Despite reports of the characteristics of air pollutants at traffic sites in Beijing, few studies have explored their adverse effects on human health in this city.

Traffic-related air pollutant exposure exerts significant impact upon public health worldwide among urban residents (Forehead and Huynh, 2018, Lelieveld et al., 2015). For example, the traffic intensity on the nearest road to a given residential area exhibited a clear association with mortality in a long-term study of a Dutch cohort (Beelen et al., 2008). The air pollutants emitted from road vehicles adversely affected pregnancy outcomes, including a lower birthweight and cardiovascular defects (Chen et al., 2008, Jacobs et al., 2017, Jiang et al., 2017). Furthermore, due to their small median diameters, road traffic-generated aerosols are able to penetrate deeply into the human respiratory system, thereby causing harmful health outcomes such as asthma attacks, chronic bronchitis, and lung cancers, hence increasing morbidity and mortality (Künzli et al., 2000, Vu et al., 2018). Yi et al., (2017) estimated the association between traffic-related air pollutants and allergic diseases in children in Seoul (South Korea) and found that a higher risk for children to develop atopic eczema. As a traffic-related air pollutant, $NO_2$ has received much attention due to its long-term effects upon all-cause mortality (Huangfu and Atkinson, 2020, Huang et al., 2021, Brimblecombe et al., 2021). In Beijing, the number of annual premature deaths attributed to traffic-related $PM_{2.5}$ exposure was estimated to be 4435 based upon weekday concentrations and 3462 based upon weekend day pollution levels (Tong et al., 2020).

Similar to other metropolitan areas, Beijing has implemented a series of policies and regulations encompassing traffic emission control to reduce roadside air pollution over the past decade, such as the Regulations of the Beijing Municipality on Atmospheric Pollution Prevention and Control, and Regulations of the Beijing Municipality on Atmospheric Pollution Prevention and Control from Motor Vehicles and Non-road Mobile machinery (GBM, 2018; BTMB, 2020). These policies mainly focus on the implementation of new vehicle emission standards and fuel standards, elimination of aging vehicles, promotion of clean-energy vehicles, and adjustment of the fleet structure and transport system by increasing public transport infrastructure.

The aim of this study was to give a comprehensive insight into roadside air pollution from 2014 to 2020 and to assess the effects of different vehicle types due to stricter traffic policies. Additionally, the adverse effects of air pollution exposure on human health were evaluated. This work firstly presents the long-term trends of air pollutants at five roadside monitoring stations to recognize the effects of sampling environments with various vehicle volumes and types. Secondly, roadside increments of air pollutants were estimated based on measured data retrieved from roadside and urban background monitoring stations by a paired-site study. Finally, the public health impacts of traffic-related $PM_{2.5}$, $NO_2$ and $SO_2$ emissions were estimated and are discussed.

## 2. Materials and methods

### 2.1. Data selection and analysis

Since 2013, the concentrations of six major air pollutants ($PM_{2.5}$, $PM_{10}$, $NO_2$, $SO_2$, CO and $O_3$) in Beijing have been observed at 35 air quality monitoring stations with automated monitoring systems and are presented on the website of the Beijing Municipal Ecological and Environmental Monitoring Center (http://www.bjmemc.com.cn/). These monitoring stations include 12 urban background sites, 11 suburban sites, 7 rural sites and 5 traffic sites (as shown in Figure 1). In this study, the datasets of the traffic and urban background sites during 2014 to 2020 were downloaded from http://beijingair.sinaapp.com. The hourly concentrations of $PM_{2.5}$ and $PM_{10}$ covered the period from January 1 2014 to December 31 2020 and the values of the other components covered April 1 2014 to December 31 2020. The concentration levels exceeding three times the median value over all similar characterized sites were suspected as outlier data points. Those data which lasted for less than three hours and exceeded the previous concentrations by more than tenfold were deleted. These were few, and the effect on mean concentrations was negligible.

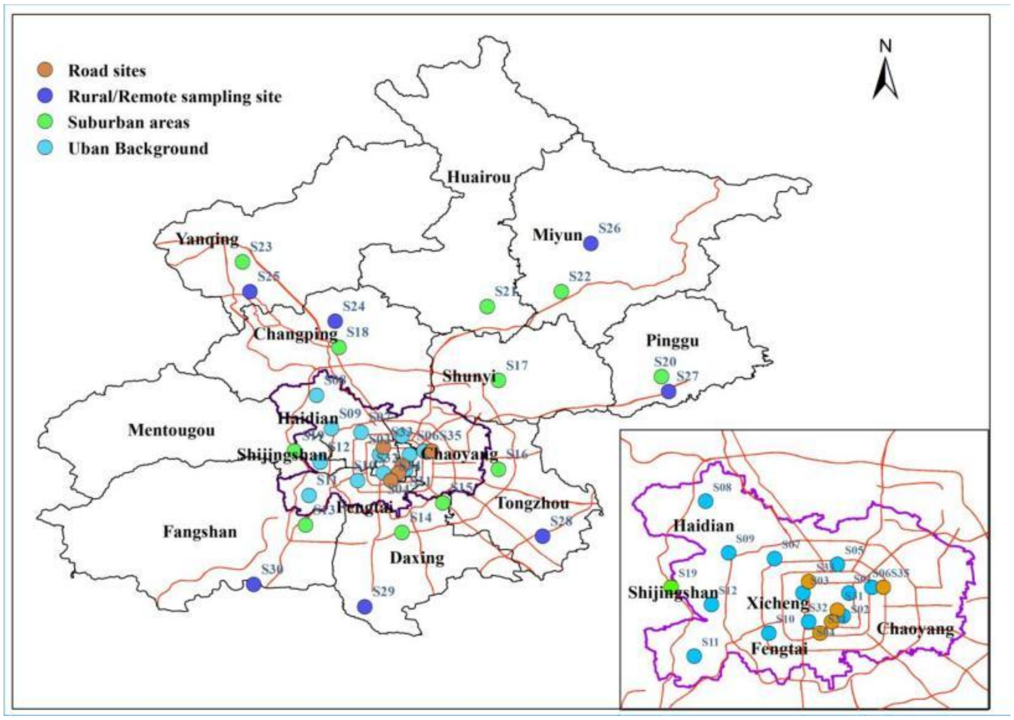


**Figure 1**. Map of the 35 air quality monitoring stations in Beijing. The orange lines represent the main highways in Beijing.

Based on the characteristics of the monitoring sites with various vehicle volumes and types, the five traffic sites were divided into three groups (Harrison et al., 2021b). The first group contains Qianmen station, Yongdingmen Inner Street station and Xizhimen North Street station, which represent inner city streets with a majority of light-duty gasoline vehicles. Secondly, the South 3$^{rd}$ Ring Road station represents a typical arterial highway with a high loading of diesel trucks. There are normally several bus stations near the monitoring station and the road width is 60 m with a high vehicle volume. Thirdly, the East 4$^{th}$ Ring Road station locates near a highway with a high loading of diesel vehicles due to several nearby large warehouses. This station is located along the East 4$^{th}$ Ring Road with a surrounding environment comprising parks and business areas, and there is a high vehicle volume with a 67 m road width.

Roadside increments were calculated by subtracting the concentrations of air pollutants at urban background monitoring stations from those observed at the roadside monitoring sites. This difference represents the influence of traffic in an urban area above the air quality from the urban background. It was calculated as follows.

$$\Delta C_i = C_{i,\,road} - C_{i,\,urban} \quad (1)$$

where $\Delta C_i$ is the road increment of type i air pollutant; $C_{i,\,road}$ is the pollutant i concentration at the roadside monitoring site; and $C_{i,\ urban}$ is the pollutant i concentration at the urban background site.

For an individual site, $\Delta C_i$ was calculated by subtracting the air pollutant level at nearby urban background site from the air pollutant concentration at the traffic site. For the whole of Beijing, the $\Delta C_i$ was averaged by the roadside increments of air pollutant i at five traffic monitoring sites.

**2.2. Calculations of the health impacts attributable to the traffic-related air pollutants**

Many studies have applied various methods to calculate the impact of long-term exposure to fine particles, nitrogen dioxide, sulphur dioxide and ozone on all-cause premature mortality (Burnett et al., 2014; Cohen et al., 2017; Jerrett et al., 2009; Turner et al., 2016; Yin et al., 2017). The attributable mortality or disability adjusted life years (DALYs) have been estimated based on detailed estimates of the exposure concentration and application of exposure-response functions. In this study, we estimated the premature mortality and acute morbidity attributable to traffic-related $PM_{2.5}$ via the exposure-response (ER) function. Moreover, we calculated the relative public health effects of pairs of air pollutants based on the relative risk of the attributable mortality as derived from previous studies in China.

The concentrations of $PM_{2.5}$ from a dispersion simulation on urban roads in Beijing were estimated by the urban air pollution dispersion and chemistry model ADMS-Urban, based on the $PM_{2.5}$ emission inventory of exhaust vehicles. ADMS-Urban is a quasi-Gaussian pollution dispersion and chemistry model that has been widely applied for assessment of emission control strategies and simulation of the dispersion of air pollutants (e.g. Biggart et al., 2020; Cui et al., 2022).

On the basis of the population data (https://www.worldpop.org/geodata/summary?id=3487 3), mortality and morbidity baseline (National Health Commission of China, 2015 & 2021) in for each year, the acute morbidity and premature deaths attributable to traffic-related $PM_{2.5}$ exposur e were calculated using a Poisson regression model as follow.

$$P_{tra} = P_{total} \times \frac{EXP(\beta \times C_{tra}) - 1}{EXP(\beta \times C_{tra})} \times I_0 \tag{2}$$

where $P_{tra}$ is the number of premature deaths due to traffic-related $PM_{2.5}$; $P_{total}$ represents the total population in Beijing; β is the beta coefficient from a log-linear model indicating changes in all-cause mortality and respiratory morbidity per unit concentration, which is 5.4‰ and 5‰, respectively, from the previous studies (Fang et al., 2016; Tong et al., 2020); $C_{tra}$ refers to the exposure concentration of population-weighted traffic-related $PM_{2.5}$. $I_0$ denotes the baseline mortality and morbidity rates in Beijing.

In order to assess the relative public health effect of $NO_2$, $SO_2$ and $PM_{2.5}$, we followed the methods of Harrison and Beddows (2017), who first considered two pollutants in the same model and compared the effects of $PM_{2.5}$ and $NO_2$ originating from traffic on the premature mortality in London. They applied the Hazard Ratio coefficients for $PM_{2.5}$ and $NO_2$ that were recommended by the World Health Organization (WHO) Health Risks of Air Pollution in Europe (HRAPIE) project to assess the mortality impact of traffic-related $NO_2$ and $PM_{2.5}$, which increased from 2010 to 2015. We collected the Hazard Ratios for air pollutants, thereby obtaining possible results from previous studies in China, for each 10 μg $m^{-3}$ increment in China, respectively, which is described in detail in the Supplementary. The Hazard Ratios for annual mean $PM_{2.5}$, $NO_2$ and $SO_2$ exposure and natural-cause mortality were 1.11 (95% CI: 1.08-1.14), 1.06 (95% CI: 1.01-1.04) and 1.105 (95% CI: 1.022-1.195).

The relative health impact on the all-cause mortality was calculated as follows.

$$RHI_{i,j,r} = \frac{\Delta C_{i,r}}{\Delta C_{j,r}} \times \frac{MI_i - 1}{MI_j - 1} \quad (3)$$

where $RHI_{i,j,r}$ is the relative health impact of air pollutants i and j in year r; $\Delta C_{i,r}$ and $\Delta C_{j,r}$ are the road increments of air pollutants i and j, respectively, in year r; and $MI_i$ and $MI_j$ are the Hazard Ratios per unit mass, which represent the all-cause mortality impact of air pollutants i and j. In this study, i refers to the $NO_2$ or $SO_2$, and j represents $PM_{2.5}$, and r is the year from 2014 to 2020.

Here we just focused the relative health effect of the traffic-related air pollutants, such as $PM_{2.5}$, $NO_2$, and $SO_2$ based on their road incremental concentration of pollutants. For $O_3$, it is mostly titrated by the fresh NO emitted from road traffic at roadside, so the road traffic emissions are a sink for ozone, and hence the roadside increment is negative for $O_3$ (See Figure 2). The corresponding public health risk of ozone with other air pollutants is significantly reduced due to the titration effect of NO at roadside. Therefore, we did not include ozone in our assessment of health impacts.

## 3. Results

### 3.1. Long-term trends of the air pollutants in the roadside environment of urban Beijing

The average mass concentrations of $PM_{10}$, $PM_{2.5}$, $NO_2$, $SO_2$, CO and $O_3$ from 2014 to 2020 at five roadside monitoring sites were 101.1 μg $m^{-3}$, 68.3 μg $m^{-3}$, 65.3 μg $m^{-3}$, 11.0 μg $m^{-3}$, 1.1

mg m$^{-3}$, and 46.1 μg m$^{-3}$, respectively. These levels were higher than those at urban background sites, except for ozone, which were 94.4 μg m$^{-3}$, 63.0 μg m$^{-3}$, 45.8 μg m$^{-3}$, 8.6 μg m$^{-3}$, 1.0 mg m$^{-3}$, and 59.2 μg m$^{-3}$, respectively. The spatial pattern indicated that the $NO_2$ level in the city was largely affected by traffic emissions, but the $PM_{2.5}$ level was largely affected by a large background from regional transport of air pollution (Figure S1 and S2). This result reflected the fact that traffic is a significant source for the air pollutants in the city, which was verified by the significant correlations of $NO_2$ and other air pollutants (Figure S3). As shown in Table 1 and Figure 2, the observations demonstrate that air pollutant concentrations have decreased significantly by 47% to 71% between 2014 and 2020. For example, the mean value of $PM_{2.5}$ in 2020 was almost 40% lower than that observed in 2014. Moreover, there was a remarkable decrease for other air pollutants, such as 4.4-20.0% a$^{-1}$ for $PM_{10}$, 2.4-22.9% a$^{-1}$ for $NO_2$, 10.2-39.7% a$^{-1}$ for $SO_2$, and 10.4-18.2% a$^{-1}$ for CO. On the contrary, ozone increased by 17.4% during this period. The gradual decrease of these air pollutants is primarily attributed to the implementation of a series of policies and regulations on traffic emission control and management (Vu et al., 2019). Whereas Vu et al. (2019) used the Random Forest machine learning algorithm to reduce the impact of both seasonal and weather variations in this study, the trends have not been deweathered as this had only modest effects and the current dataset is longer, giving less scope for influences from inter-annual variability of weather. It should also be noted that although data are reported for 2020, these are likely to be anomalous due to the significant effect of the COVID-19 lockdown (Cao et al., 2021, Shi et al., 2021), which is comparable with the findings at Wuhan, Daegu and Tokyo during this period (Ma et al., 2020).

**Table 1**. Concentration of the air pollutants (mg m$^{-3}$ for CO and μg m$^{-3}$ for others) and the decrease in concentration relative to the previous year (% a$^{-1}$) during 2014-2020.

| Year | $PM_{2.5}$ | | $PM_{10}$ | | $NO_2$ | | $SO_2$ | | CO | | $O_3$ | |
|---|---|---|---|---|---|---|---|---|---|---|---|---|
| | Conc. | % decrease | Conc. | % decrease | Conc. | % decrease | Conc. | % decrease | Conc. | % decrease | Conc. | % decrease |
| 2014 | 98.2 | | 132.7 | | 82.0 | | 16.1 | | 1.4 | | 45.9 | |
| 2015 | 90.4 | 8.0 | 126.9 | 4.4 | 75.6 | 7.8 | 17.6 | -9.1 | 1.5 | -9.0 | 42.3 | 7.8 |
| 2016 | 80.8 | 10.6 | 106.8 | 15.8 | 69.8 | 7.7 | 13.9 | 20.8 | 1.3 | 11.5 | 44.0 | -4.0 |
| 2017 | 67.6 | 16.3 | 91.8 | 14.1 | 68.1 | 2.4 | 12.5 | 10.2 | 1.1 | 17.3 | 42.1 | 4.5 |
| 2018 | 55.7 | 17.6 | 94.5 | -3.0 | 64.5 | 5.3 | 7.5 | 39.7 | 0.9 | 18.2 | 46.4 | -10.2 |
| 2019 | 46.1 | 17.3 | 75.6 | 20.0 | 55.4 | 14.0 | 6.0 | 20.9 | 0.8 | 10.4 | 48.4 | -4.3 |
| 2020 | 39.9 | 13.4 | 66.6 | 11.9 | 42.7 | 22.9 | 4.5 | 23.9 | 0.7 | 11.3 | 51.5 | -6.5 |

Conc. means concentration.

Figure 2 further presents the seasonal variation in the monthly values of air pollutants at traffic sites and urban background sites. Except for ozone, the traffic sites attained higher values than those at urban background sites in most months. $PM_{2.5}$ concentrations were higher in winter (traffic sites: 83.2 μg $m^{-3}$; urban background sites: 76.8 μg $m^{-3}$) and lower in summer (traffic sites: 52.6 μg $m^{-3}$; urban background sites: 49 μg $m^{-3}$), followed by those in fall and spring. This result corresponds with the findings in urban Beijing obtained by Xu and Zhang (2020). $SO_2$ and CO trends were similar to that of the $PM_{2.5}$ concentration. The highest $PM_{10}$ concentrations (traffic sites: 117.7 μg $m^{-3}$; urban background sites: 114.2 μg $m^{-3}$) were observed during spring, followed by winter, fall, and summer. The highest concentration of $PM_{10}$ in spring may be attributable to the significant contribution of Asian dust that is transported from North China during spring (Liu et al., 2014). There is a minor seasonal fluctuation for $NO_2$ at the traffic sites (range: 60.8 to 68.5 μg $m^{-3}$), but the $NO_2$ data appeared to indicate higher values in winter and fall, at approximately 52 μg $m^{-3}$, and a lower level in summer (33.9 μg $m^{-3}$) at the urban background sites. In contrast, the highest level of ozone was found in summer.

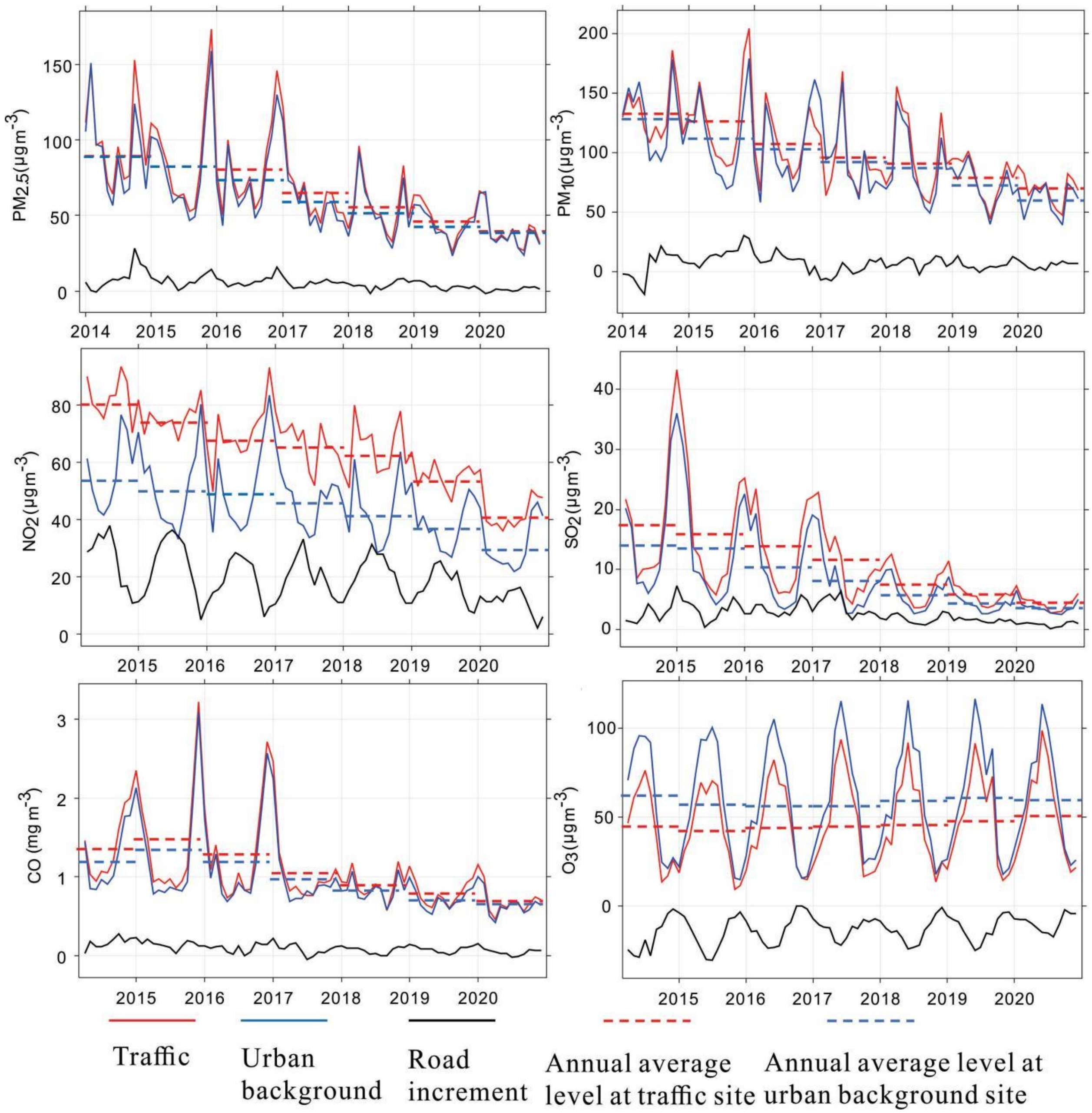


**Figure 2**. Monthly mean concentration trends of air pollutants at the traffic sites and urban background monitoring sites, and the roadside increment. The pollutant values at the traffic sites are calculated as the average value over the five traffic monitoring sites. The pollutant levels at urban background sites are calculated as the average value from twelve urban background monitoring sites

Diurnal variations of air pollutants at traffic sites and urban background sites during 2014 to 2020 are shown in Figures 3 and 4, respectively. Generally, higher levels of air pollutants were observed at nighttime rather than in daytime, indicating that mixed boundary layers and low temperature highly influence the daily patterns of pollutants (Zhong et al., 2017). The highest $NO_2$ concentration at the traffic sites was observed earlier than that at urban background sites. A weak peak was observed in the morning (7:00-9:00 am) which is a typical high emission period due to the traffic rush hour. The lowest values of these air pollutants were observed during 5:00 to 6:00 am and 12:00 to 16:00 pm. On the contrary, the peak of concentrations for $SO_2$ and ozone occurred during daytime. Additionally, the difference between the highest and lowest values at traffic sites was approximately 22% greater than that at urban background sites, suggesting that the $NO_2$ concentration in the ambient environment was significantly affected by traffic.

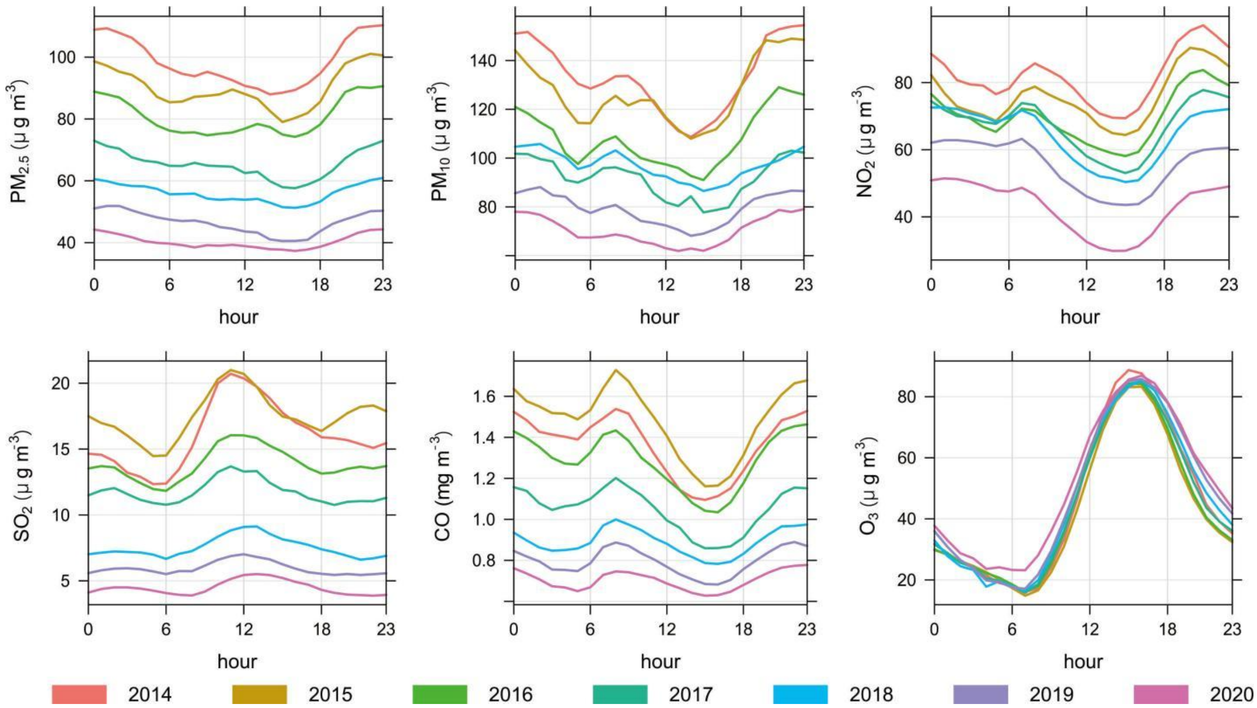


**Figure 3**. Diurnal variation of components at traffic sites during 2014 to 2020.

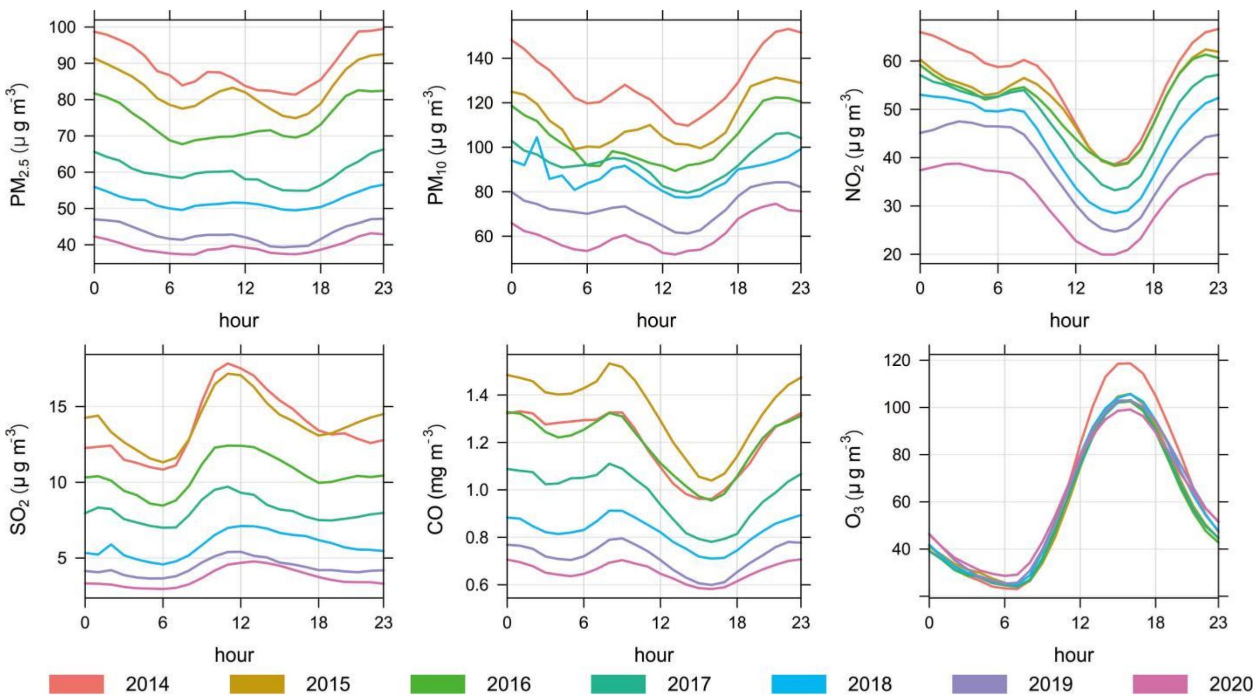


**Figure 4**. Diurnal variation of components at urban background sites during 2014 to 2020.

### 3.2. Comparison of different traffic monitoring sites

The air pollutant levels at the South 3rd Ring Road station were higher than those at the Street stations and the East 4th Ring Road station during 2014 to 2020 as presented in Figure 5. For instance, the $PM_{2.5}$ concentrations at the South 3rd Ring Road were 5.9 to 9.9 μg $m^{-3}$ higher than those in the Street stations and 3.8 to 8.2 μg $m^{-3}$ higher than those at the East 4th Ring Road during 2014 to 2017. On the contrary, $PM_{2.5}$ values at these stations were similar during 2018 to 2020, which showed a similar trend with the $SO_2$. $PM_{2.5}$ and $SO_2$ concentrations at these three groups of sites indicated a statistically significant difference ($p<0.001$) between street sites and South 3rd and East 4th Ring Road stations. The other air pollutants at these sites also exhibited a statistically significant difference ($p<0.001$). Based on the Theil-Sen estimator, the overall trend of air pollutants at the South 3rd Ring Road station, as shown in Figure 5, decreased more than those at the other stations every year. The values of $PM_{10}$ at the South 3rd Ring Road were also mostly higher than that at Street stations (11.0 to 26.8 μg $m^{-3}$ higher), but were comparable to that on the 4th Ring Road. This result suggests that non-exhaust emissions, including road surface and resuspended dust, and wear of the brakes and tyres, contributed to coarse particles. This is attributed to the larger number of heavy duty vehicles on highways than that on the urban streets, which produce high non-exhaust emissions. $NO_2$ was mainly influenced by vehicles, and was the highest in the South 3rd Ring Road (109.8 to 47.6 μg $m^{-3}$). There is a clearly decreasing trend for the $NO_2$ level from 2014 to 2020 at these stations, indicative of the remarkable achievement in Beijing's traffic air quality improvement after implementing a series of regulations on traffic emission control from 2013. Regarding CO, the South 3rd Ring Road also had CO concentrations 0.05 to 0.3 mg $m^{-3}$ higher than that at Street stations and the 4th Ring Road. This probably results from the higher traffic volume. However, the concentration of $O_3$ was highest in the Street stations (45.8 to 54.2 μg $m^{-3}$), followed by the 4th Ring road (32.9 to 46.7 μg $m^{-3}$) and South 3rd Ring road (27.7 to 49.5 μg $m^{-3}$). The $O_3$ values were higher in summer and lower in winter, and show a gradual increase from 2014 to 2020.

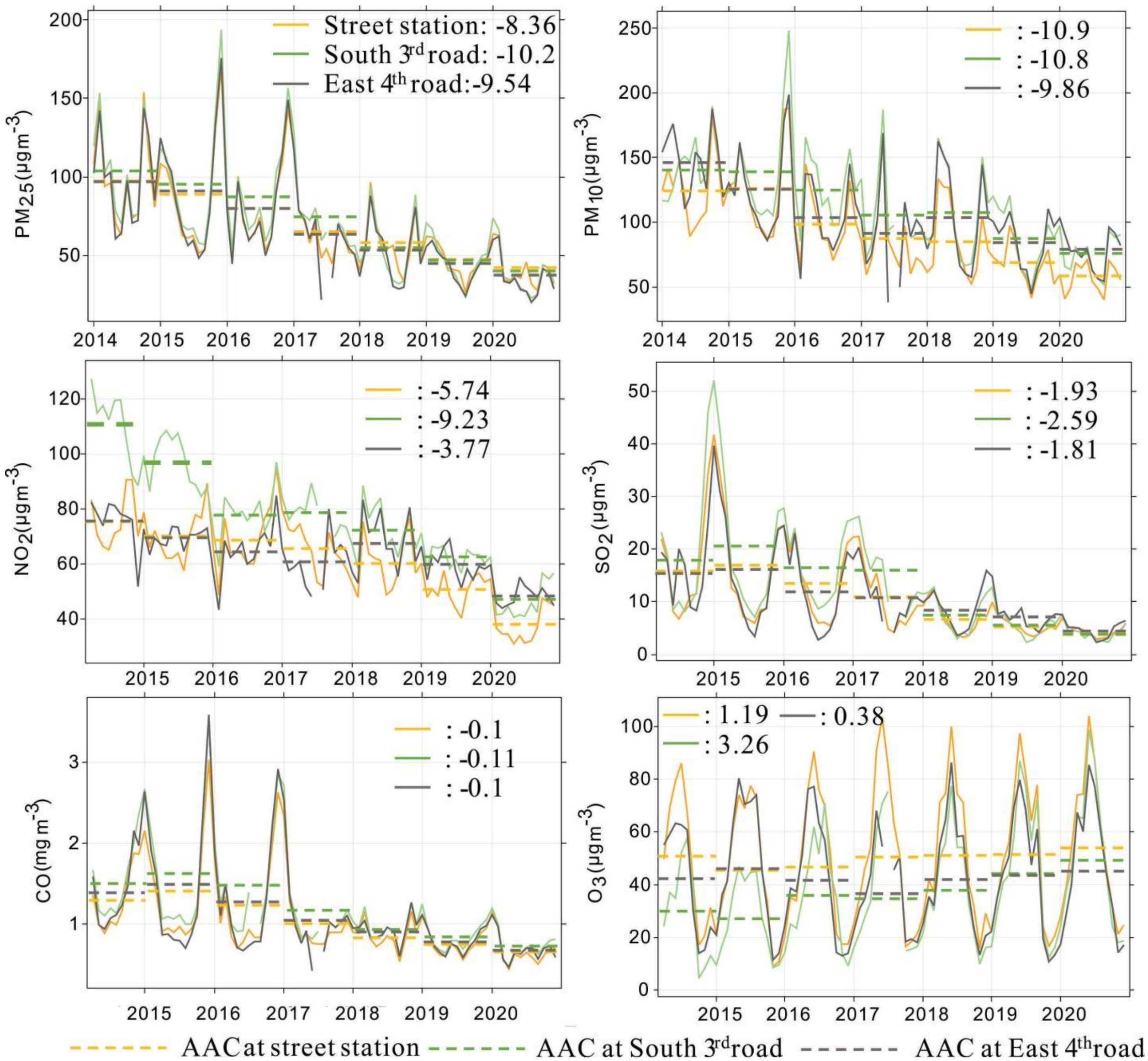


**Figure 5**. Trend of the monthly mean pollutant concentration at traffic monitoring stations. The numbers shown in the figure represent the overall trend of air pollutant level (μg $m^{-3}$ $a^{-1}$) by

Theil-sen estimator. AAC refers to the annual average concentration.

### 3.3. Long-term trends of roadside increment of air pollutants.

The roadside increments and their percentage increases above urban background concentrations of air pollutants in Beijing for the period of 2014 to 2020 are summarized in Table 2 and Figure 6. The highest annual mean roadside increment when expressed as a concentration was found for CO (95.7 μg $m^{-3}$), followed by $NO_2$ (19.5 μg $m^{-3}$), $PM_{2.5}$ (5.3 μg $m^{-3}$) and $SO_2$ (2.4 μg $m^{-3}$), which is lower than those observed in London and Hong Kong during 2016 to 2018 which is also a metropolis with a high vehicle volumes and has implemented many policies to reduce the traffic-related air pollutants (Harrison et al., 2021). It clearly indicates that vehicle exhaust is a significant source of CO and $NO_2$ in urban Beijing. $PM_{2.5}$ roadside increments experienced an obvious decrease from 2014 (9.4 μg $m^{-3}$) to 2020 (0.9 μg $m^{-3}$), and the percentage increase above urban background values by traffic decreased from 16.8% in 2014 to 3.5% in 2020. In the case of $NO_2$, the increments due to traffic and the percentage increment above urban background presented a smaller change during this period compared with the $PM_{2.5}$ and CO. It appears that the upgrades to the vehicle fleet over this period had greater benefits for $PM_{2.5}$ emissions than for oxides of nitrogen, although this may be an artefact of the non-linear relationship between $NO_x$ and $NO_2$. Measurements at a roadside site in London show little change in $NO_2$ despite a substantial reduction in $NO_x$ (Krecl et al., 2021) The roadside increments of $PM_{2.5}$, $NO_2$ and $SO_2$ were approximately 30-50% higher at the South 3rd road than those at the East 4th road and Street sites during 2014 to 2017, but the levels of air pollutant at these sites presented similar concentrations during 2018 to 2020.

**Table 2**. Roadside increment (ΔC) (μg $m^{-3}$) and percentage increment of roadside concentration of air pollutants above that of urban background concentration from 2014 to 2020 (% increase).

| Year | $PM_{2.5}$ | | $PM_{10}$ | | $NO_2$ | | $SO_2$ | | CO | | $O_3$ | |
|---|---|---|---|---|---|---|---|---|---|---|---|---|
| | Conc. | % increase | Conc. | % increase | Conc. | % increase | Conc. | % increase | Conc. | % increase | Conc. | % increase |
| 2014 | 9.4 | 16.8 | 3.6 | 6.5 | 26.4 | 68.4 | 2.3 | 35.7 | 164.2 | 15.5 | -17.2 | -20.9 |
| 2015 | 7.1 | 12.7 | 14.4 | 20.9 | 23.7 | 67.1 | 3.5 | 41.1 | 143.4 | 13.2 | -15.1 | -29.4 |
| 2016 | 6.7 | 13.1 | 10.3 | 16.6 | 18.6 | 51.5 | 3.3 | 51.0 | 95 | 9.5 | -12.3 | -11.9 |
| 2017 | 5.4 | 12.8 | 2.3 | 7.2 | 19.2 | 56.3 | 3.7 | 73.9 | 72.1 | 9.4 | -12.0 | -26.7 |
| 2018 | 4.0 | 12.5 | 7.5 | 16.0 | 20.8 | 70.2 | 1.7 | 39.4 | 65.9 | 9.5 | -13.5 | -21.5 |
| 2019 | 3.4 | 10.1 | 5.8 | 15.5 | 16.7 | 66.4 | 1.6 | 47.8 | 78.6 | 12.0 | -12.3 | -23.2 |
| 2020 | 0.9 | 3.5 | 5.8 | 23.6 | 11.3 | 53.5 | 0.8 | 28.8 | 47.6 | 8.0 | -9.2 | -15.2 |

Conc. denotes the concentration.

$(\%\ \text{increase} = (\Delta C_i / C_{i,\ urban}) \times 100$

Average roadside increments during 2014-2020 accounted for 7.7% and 7.2% of the total mass concentrations of $PM_{2.5}$ and $PM_{10}$, respectively, at the traffic sites. The highest increment of fine particles was found in fall and winter, which could be attributed to poorer dispersion of primary emissions. There is an opposite trend in the temporal variation of $NO_2$ and $O_3$ roadside increments, as shown in Figure 6. Higher roadside increments of $NO_2$ were found in summer, but the roadside increment of $O_3$ reached a peak in winter. The difference between the monthly variation of road increments of $O_3$ and $NO_2$ probably results from the complex reactions between $NO_2$-$NO_x$-$O_3$ yielding the different concentrations of secondary $NO_2$ and $O_3$ depending upon the occurrence of NO emitted from road vehicle exhaust and photochemistry. Figure S4 shows the polar plots of roadside increment of air pollutants by year. It seems that the decrease in the case of $PM_{2.5}$, $PM_{10}$, $NO_2$ and CO in Beijing was linked to prohibition of trucks and old vehicles from entering the city within the Sixth Ring Road during daytime since 2014. It is confirmed by a distinct peak of $NO_2$ in the late evening as shown in Figure 3. Similarly, the temporal trend of roadside increment of $SO_2$ also had an obvious decrease from 2018.

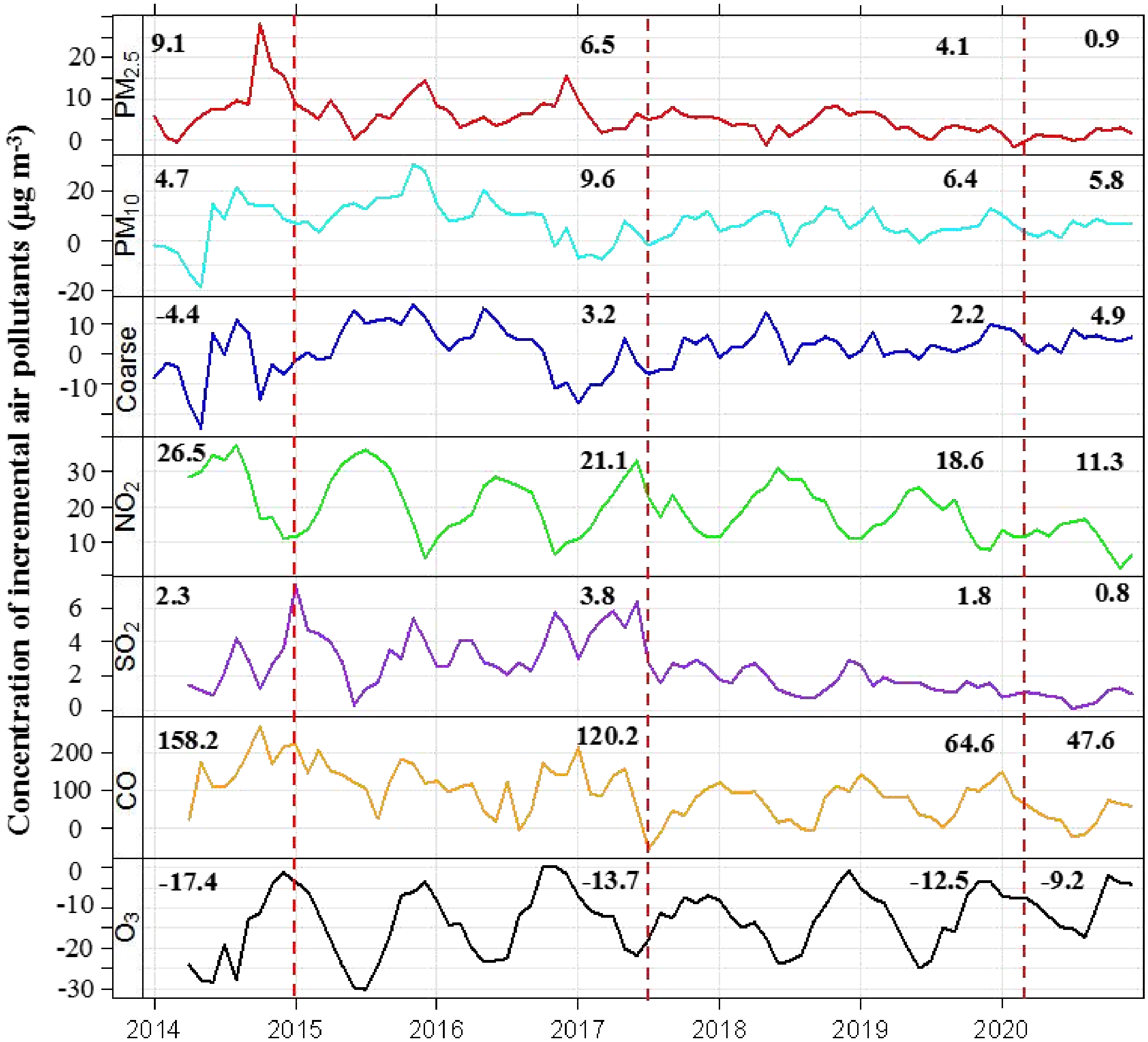


**Figure 6**. Trend of the roadside increment in Beijing during 2014-2020. The numbers in the figure indicate the road increments during different periods under the various policies.

# 4. Discussion

## 4.1 Discussion on the improvement of air quality at traffic sites

The concentrations of air pollutants in both the roadside and urban environment exhibited a substantial decrease from 2014 to 2020 in Beijing, clearly indicative of the effectiveness of air pollution control measures. Road traffic contributed to a notable roadside increment of $NO_2$ above the urban background, and the $NO_2$ at roadside sites declined the most at the South 3$^{rd}$ Ring Road and Street stations, and $NO_2$ at East 4$^{th}$ had a slightly decrease during this period. This may be the result of the low emission zone program from 2016 in central urban Beijing. The gradual decreases of $PM_{2.5}$, $PM_{10}$, CO, and $SO_2$ in the roadside atmosphere were not only driven by the reduction of emissions from vehicles, but also caused by the reduction of other combustion sources, such as industry and power plants (Zhang et al., 2019a). Ozone is a secondary pollutant that is affected by several factors. The dominant factor is the $NO_x$-$O_3$ photochemical steady state, as the reduction of traffic-related NO has led to increases in $O_3$ due to reduced $O_3$ titration (Shi et al., 2021). PCA and cluster analysis showed that low wind speed, high temperature and relative humidity promote the accumulation of $O_3$ (Table S1 and Figure S5) (Guo et al., 2017, Xue et al., 2014).

Roadside increments as calculated using a paired-site approach at different monitoring sites in Beijing could be subject to artefacts if other sources influence the measuring site. Long-term datasets and consideration of multiple sites, however, should minimise this effect. Due to the characteristics of the different monitoring sites and different traffic volumes, the roadside increments measured at the five sites represent a range of behaviours, but all show a consistent pattern. The results reported above indicate that roadside increments of $PM_{2.5}$ diminished appreciably from 2014 to 2020 in Beijing, which could be explained by the reduced primary emissions of fine particles and associated gaseous precursors originating from vehicles. In the case of $NO_2$, the roadside increment declined slightly and showed a similar trend before 2019 with a higher level in summer and lower level in winter. It is likely that $NO_x$ declined more than $NO_2$, but the data are not available to verify this.

The downward trends of the $PM_{2.5}$, $SO_2$ and CO concentrations in Figure 2 showed a breakpoint from 2017, and the rate of decline increased to 16.3%, 10.3% and 17.3% comparing with 2016. This phenomenon is likely attributable to the implementation of a new China VI fuel standard in January 2017 and the prohibition of China I and II standard light-duty vehicles from entering the central zone within the Fifth Ring Road (which includes the traffic roadside monitoring sites) after February 2017. Additionally, the implementation of the China V standard for all spark ignition vehicles in July 2015 and the increased electrification of the vehicle fleet in Beijing contributed to the decline of $PM_{2.5}$ and CO. As shown in Tables S2 and S3, the proportion of China V vehicles in Beijing reached around 50% from 2017, and the emission limits of China V and VI for PM and CO originating from the vehicles were reduced, and ultra-low sulphur fuels were adopted for all vehicles from 2017 in the cities surrounding Beijing. Meanwhile, China set up a no-coal zone in cities around Beijing from November 2017, which may also have contributed to the reduction of the $PM_{2.5}$ and $SO_2$ in roadside air, but also in the urban background. Based on Figure 6, the roadside increments of $PM_{2.5}$, $NO_2$ and CO could be divided into four periods: the first period of 01/2014-01/2015, the second period of 01/2015-06/2017 (implementation of China V standard), the third period of 07/2017-12/2019 (introduction of China VI vehicle and China VI fuel standard), and the period after 2020 which was affected by the COVID-19 lockdown and prohibition of China III diesel trucks from entering Beijing. The introduction of these policies is already having a very significant benefit for air quality. For example, roadside increments of $PM_{2.5}$, $NO_2$, $SO_2$ and CO during the third period were 4.1 $\mu g\ m^{-3}$, 18.6 $\mu g\ m^{-3}$, 1.8 $\mu g\ m^{-3}$ and 64.6 $\mu g\ m^{-3}$, versus those of 6.5 $\mu g\ m^{-3}$, 21.1 $\mu g\ m^{-3}$, 3.8 $\mu g\ m^{-3}$ and 120.2 $\mu g\ m^{-3}$ during second period, respectively. It reveals that the implementation of the new vehicle standards (Sun et al., 2021) was highly effective in terms of reduction of the roadside increments for CO (59.1%), $PM_{2.5}$ (54.8%), $NO_2$ (29.8%), $SO_2$ (20.6%). The change for the $NO_2$ was relatively limited, possibly due to the non-linearity between $NO_x$ and $NO_2$ concentrations. These control policies were found not to affect the roadside increment of coarse particles ($PM_{2.5-10}$) (see Figure 6) which arise largely from non-exhaust sources (Thorpe and Harrison, 2008) and were not subject to additional controls. On the other hand, the decrease of air pollutants from 2020 was due to the reduction of traffic flow (decrease by 7.5% with 2019) in Beijing due to the COVID-19 lockdown.

### 4.2. Relative public health impacts of traffic-related $PM_{2.5}$, $NO_2$ and $SO_2$

In Beijing, traffic emissions have significantly contributed to the air pollutants that have an influence on public health (Lei et al., 2012; Tong et al., 2020). Based on the ADMS simulation, the annual average $PM_{2.5}$ population weighted concentration from vehicle emissions is 8.0 $\mu g\ m^{-3}$ and 1.56 $\mu g\ m^{-3}$ in 2014 and 2020, respectively (Figure 7), which is similar to the $PM_{2.5}$ level estimated from the paired-site method and comparable with the results simulated by Tong et al. (2020). The annual attributable premature mortality due to traffic-related $PM_{2.5}$ was calculated by the ER function, which was 8379 cases (CI: 3686, 7586) in 2014, while an obvious decrease in health effect occurred in 2020 with 1908 (CI: 1217, 2533) cases due to much reduced $PM_{2.5}$ emissions from vehicles. Among the total premature deaths, the number within the Fifth Ring Road accounted for 58.5% in 2014, which were 688, 1219, 1388 and 1608 cases within the 2$^{nd}$ Ring Road, 2$^{nd}$ - 3$^{rd}$, 3$^{rd}$ - 4$^{th}$, and 4$^{th}$ -5$^{th}$ Ring Road, respectively, resulting from the lower population in the city center. By comparison, the proportion of premature deaths due to traffic-related $PM_{2.5}$ within the Fifth Ring Road slightly decreased to 50% in 2020. For the case of the acute morbidity from respiratory diseases due to $PM_{2.5}$, the incidence in 2014 with 461479 cases was higher than that in 2020 with 93045, illustrating another aspect of the severe public health burden of traffic-related $PM_{2.5}$. As mentioned above, a series of policies have been implemented to reduce the emissions of air pollutants from vehicles from 2013, resulting in the reduction of health burden.

In addition, the relative public health impacts of traffic-related $PM_{2.5}$ $NO_2$ and $SO_2$ were approximated according to their effect on all-cause mortality based on an exposure-response function during different time periods. The ratio of premature mortality impact per unit mass for $NO_2$ and $PM_{2.5}$ calculated from the Hazard Ratios is 0.27. The ratio of mortality impact for $SO_2$ and $PM_{2.5}$ is 0.95 for a unit mass of each. When the relative impact of two traffic-related pollutants is to be estimated, the relative concentrations of these two pollutants arising from traffic should be taken into account, as in equation (3). As a result, the ratio of all-cause mortality owing to road traffic-related $NO_2$ relative to $PM_{2.5}$ ranged from 0.76 to 0.97 in 2017, and reached 1.32 in 2019, which is presented in Figure S6. Meanwhile, the ratio for mortality caused by the $SO_2$ relative to $PM_{2.5}$ is 0.23 in 2014, and 0.44-0.65 during 2015-2019. This analysis may underestimate the effects of $NO_2$ as it uses a ratio of $NO_2/PM_{2.5}$ derived from roadside measurements, whereas the $NO_2/NO_x$ ratio typically increases with greater dilution away from roadside, an effect explicitly accounted for by Harrison and Beddows (2017) who had $NO_x$ data as well as $NO_2$ from roadside and background sites. It indicates that the premature mortality impact of traffic-related $NO_2$ is now comparable to, or may exceed the impact of $PM_{2.5}$ from traffic. The influence of traffic-related $SO_2$ upon mortality was markedly less. As shown in Figure S7, the traffic-related nitrogen dioxide and sulphur dioxide relative to $PM_{2.5}$ at street stations yielded a similar relative impact to that at the South 3$^{rd}$ and East 4$^{th}$ Ring Road site before 2018, indicating that the effect of $NO_2$ on premature mortality was of a similar magnitude to that of $PM_{2.5}$, but greater than that of $SO_2$. However, the trend changed afterwards. The effect of $NO_2$ and $SO_2$ at the East 4$^{th}$ Ring Road on public health relative to $PM_{2.5}$ increased faster than at the other two sites, which was due to the prohibition of diesel trucks entering the inner city.

Although strict control measures have been applied to vehicle emissions, the impact of air pollutants on human health has a significant variation according to the vehicle types and fuel. Shi et al. (2021) concluded that the decline in $NO_2$ concentrations attributable to the COVID-19 lockdown which introduced severe restrictions on road traffic was not as notable as expected in China. This is consistent with the result from Grange et al. (2017), who analysed $NO_x$ and $NO_2$ hourly concentrations spanning 130 million hours retrieved from roadside monitoring stations in Europe and found that the roadside $NO_2$ level declined due to reduced emissions of $NO_x$ much less than expected due to the increasing usage of diesel vehicles in Europe. According to the Emissions Inventory in 2021 (Table S5), 96.5% of $PM_{2.5}$ vehicle exhaust emissions and 74% of $NO_x$ emissions were attributable to diesel vehicles in Beijing.

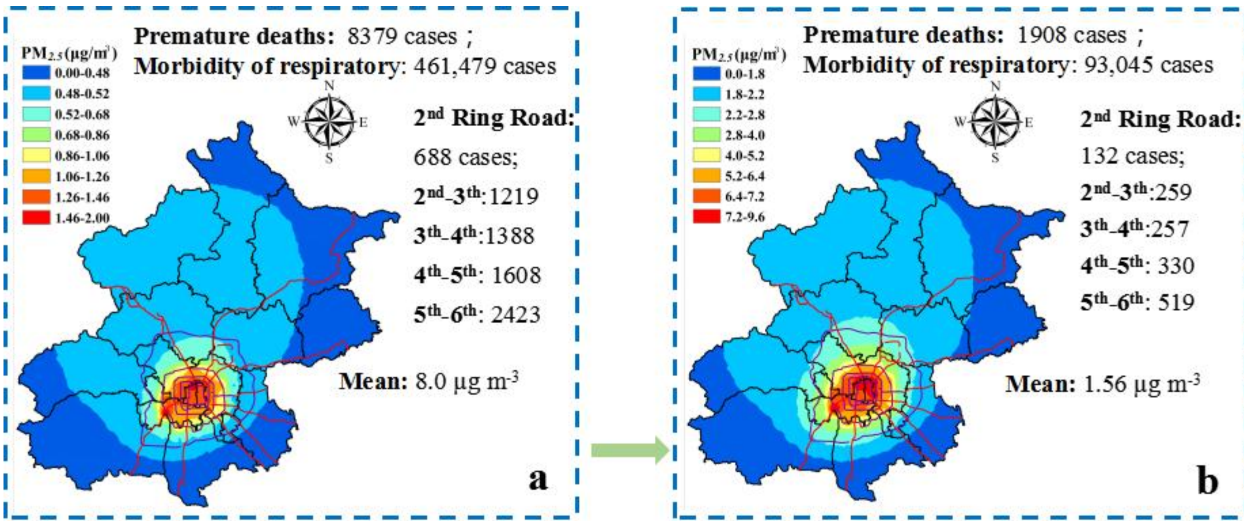


Figure 7 The spatial distribution of simulated $PM_{2.5}$ concentration from vehicles in 2014 (a) and 2020 (b). The numbers in the figure refer to the annual average $PM_{2.5}$ and the number of premature deaths in various zones.

## 5. Conclusion

In order to evaluate the characteristics of traffic-related air pollutants and consequent health impacts, this study collected hourly mass concentrations of $PM_{2.5}$, $PM_{10}$, $NO_2$, $SO_2$, CO and $O_3$ from 5 traffic sites and 12 urban background sites in Beijing during 2014 to 2020. The roadside increments of air pollutants were obtained using a paired-site approach. As a result, the annual mean air pollutant concentrations are found to have diminished significantly by 47% to 71% from 2014 to 2020, specifically 4.4-20.0 % $a^{-1}$ for $PM_{10}$, 2.4-22.9 % $a^{-1}$ for $NO_2$, 10.2-39.7 % $a^{-1}$ for $SO_2$, and 10.4-18.2 % $a^{-1}$ for CO. On the contrary, the concentration of ozone increased by 17.4% during this period. In terms of the diurnal variation of air pollutants, a higher level of air pollutants was observed at nighttime than those at daytime due to a shallower mixed boundary layer and temperature. The air pollutant levels at South 3$^{rd}$ Ring Road station were higher than those at the street stations and East 4th Ring Road station during 2014 to 2020, which could be affected by the air mass passage through the area south of Beijing with its dense industry.

The roadside increments and the percentage increase above urban background values of $PM_{2.5}$, $NO_2$, $SO_2$ and CO decreased from 2014 to 2020, revealing that the implementation of new vehicle standards (China V and VI) led to reductions of air pollutants in the roadside environment, except for $PM_{10}$ and $O_3$. Based on ADMS simulated $PM_{2.5}$ dispersion model concentrations from exhaust vehicle emissions , the premature deaths due to traffic-related $PM_{2.5}$ were estimated to be 8379 and 1908 cases in 2014 and 2020, respectively. The number of $PM_{2.5}$-induced acute cases of respiratory diseases were 461479 cases in 2014 and 93045 cases in 2020, illustrating a more severe public health burden of traffic-related $PM_{2.5}$ than that reflected by mortality alone. The relative public health impacts of $PM_{2.5}$, $NO_2$ and $SO_2$ were estimated roughly from their influence on all-cause mortality. It was found that the effect of $NO_2$ from road traffic on premature mortality was of a similar magnitude to that of $PM_{2.5}$, and greater than that of $SO_2$. It indicates that further reduction of $NO_x$ emitted from traffic will likely have substantial benefits for public health.

Acknowledgement

This work was supported by the National Natural Science Foundation of China (Nos. 21806012, 42075112, and 41775127), the Basic Research Fund of the CAMS (No. 2020Z002) and the Foundation of Beijing Municipal Research Institute of Eco-Environmental Protection (No. Y2022-007).

## References

Beelen, R., Hoek, G., van den Brandt, P.A., Goldbohm, R.A., Fischer, P., Schouten, L.J., Jerrett, M., Hughes, E., Armstrong, B., Brunekreef, B. 2008. Long-term effects of traffic-related air pollution on mortality in a Dutch cohort (NLCS-AIR study). *Environmental health perspectives,* 116, 196-202.

Brimblecombe, P., Lai, Y. 2021. Subtle Changes or Dramatic Perceptions of Air Pollution in Sydney during COVID-19. *Environments*, 8(1), 2.

Biggart, M., Stocker, J., Doherty, R. M., Wild, O., Hollaway, M., Carruthers, D., Shi, Z. 2020. Street-scale air quality modelling for Beijing during a winter 2016 measurement campaign. *Atmospheric Chemistry and Physics*, 20(5), 2755-2780.

BTMB, 2020. Beijing Traffic Management Bureau (BTMB): Regulations of Beijing Municipality on Atmospheric Pollution Prevention and Control from motor vehicles and non-road mobile machinery. Available on: http://jtgl.beijing.gov.cn/jgj/jgxx/flfg/bjsfggz/1793533/index.html

Burnett, R.T., Pope III, C.A., Ezzati, M., Olives, C., Lim, S.S., Mehta, S., Cohen, A. 2014. An integrated risk function for estimating the global burden of disease attributable to ambient fine particulate matter exposure. *Environmental health perspectives*, 122 (4), 397-403.

Cai, T., Zhang, Y., Fang, D., Shang, J., Zhang, Y., Zhang, Y. 2017. Chinese vehicle emissions characteristic testing with small sample size: Results and comparison. *Atmospheric Pollution Research,* 8, 154-163.

Cao, X., Tian, Y., Shen, Y., Wu, T., Li, R., Liu, X., Yeerken, A., Cui, Y., Xue, Y., Lian, A. 2021. Emission Variations of Primary Air Pollutants from Highway Vehicles and Implications during the COVID-19 Pandemic in Beijing, China. *International Journal of Environmental Research and Public Health,* 18, 4019.

Chen, H., Namdeo, A., Bell, M. 2008. Classification of road traffic and roadside pollution concentrations for assessment of personal exposure. *Environmental Modelling & Software,* 23, 282-287.

Chen, W., Li, A., Zhang, F. 2018. Roadside atmospheric pollution: still a serious environmental problem in Beijing, China. *Air Quality, Atmosphere & Health,* 11, 1203-1216.

Chen, X., Wang, X., Huang, J., Zhang, L., Song, F., Mao, H., Chen, K., Chen, J., Liu, Y. M., Jiang, G.. 2017. Nonmalignant respiratory mortality and long-term exposure to $PM_{10}$ and

SO$_2$: A 12-year cohort study in northern China. *Environmental Pollution,* 231, 761-767.
Cohen, A. J., Brauer, M., Burnett, R., Anderson, H. R., Frostad, J., Estep, K., Forouzanfar, M. H. 2017. Estimates and 25-year trends of the global burden of disease attributable to ambient air pollution: an analysis of data from the Global Burden of Diseases Study 2015. *The Lancet*, 389 (10082), 1907-1918.
Cui, Y., Zhang, G., Wang, W., Shen, Y., Zhai, X., Wu, X., Xue, Y. 2022. Ten-year emission characteristics of atmospheric pollutants from incineration of sacrificial offerings in China. *Journal of Environmental Sciences*.
Fang, D., Wang, Q. G., Li, H., Yu, Y., Lu, Y., & Qian, X. 2016. Mortality effects assessment of ambient PM$_{2.5}$ pollution in the 74 leading cities of China. *Science of the Total Environment*, 569, 1545-1552.
Forehead, H., Huynh, N. 2018. Review of modelling air pollution from traffic at street-level-The state of the science. *Environmental Pollution,* 241, 775-786.
GBM, 2018. The People's Government of Beijing Municipality (GBM): Regulations of Beijing Municipality on Atmospheric Pollution Prevention and Control. Avaliable online: http://www.beijing.gov.cn/zhengce/zhengcefagui/201905/t20190522_61138.html
Gowers, A. M., Walton, H., Exley, K.S., Hurley, J.F. 2020. Using epidemiology to estimate the impact and burden of exposure to air pollutants. *Philosophical Transactions of the Royal Society A,* 378, 20190321.
Grange, S.K., Lewis, A.C., Moller, S.J., Carslaw, D.C. 2017. Lower vehicular primary emissions of NO$_2$ in Europe than assumed in policy projections. *Nature Geoscience,* 10, 914-918.
Guo, H., Wang, Y., & Zhang, H. 2017. Characterization of criteria air pollutants in Beijing during 2014–2015. *Environmental Research*, 154, 334-344.
Harrison, R.M., Allan, J., Carruthers, D., Heal, M.R., Lewis, A.C., Marner, B., Murrells, T., Williams, A. 2021a. Non-Exhaust Vehicle Emissions of Particulate Matter and VOC from Road Traffic: A Review. *Atmospheric Environment*, 118592.
Harrison, R.M., Beddows, D.C. 2017. Efficacy of recent emissions controls on road vehicles in Europe and implications for public health. *Scientific reports,* 7, 1-5.
Harrison, R.M., Vu, T.V., Jafar, H., Shi, Z. 2021b. More mileage in reducing urban air pollution from road traffic. *Environment International,* 149, 106329.
Huang, R., Zhang, Y., Bozzetti, C., Ho, K., CAO, J., Han, Y., Daellenbach, K.R., Slowik, J.G.,

Platt, S.M., Canonaco, F., Zotter, P., Wolf, R., Pieber, S.M., Bruns, E.A., Crippa, M., Ciarelli, G., Piazzalunga, A., Schwikowski, M., Abbaszade, G., Schnelle-Kreis, J., Zimmermann, R., An, Z., Szidat, S., Baltensperger, U., El Haddad, I., Prevot, A.S. 2014. High secondary aerosol contribution to particulate pollution during haze events in China. *Nature,* 514, 218-22.

Huang, S., Li, H., Wang, M., Qian, Y., Steenland, K., Caudle, W.M., Liu, Y., Sarnat, J., Papatheodorou, S. & Shi, L. 2021. Long-term exposure to nitrogen dioxide and mortality: A systematic review and meta-analysis. *Science of The Total Environment*, 145968.

Huangfu, P., Atkinson, R. 2020. Long-term exposure to $NO_2$ and $O_3$ and all-cause and respiratory mortality: A systematic review and meta-analysis. *Environment International,* 144, 105998.

Jacobs, M., Zhang, G., Chen, S., Mullins, B., Bell, M., Jin, L., Guo, Y., Huxley, R., Pereira, G. 2017. The association between ambient air pollution and selected adverse pregnancy outcomes in China: a systematic review. *Science of the Total Environment,* 579, 1179-1192.

Jerrett, M., Burnett, R. T., Pope III, C. A., Ito, K., Thurston, G., Krewski, D., & Thun, M. 2009. Long-term ozone exposure and mortality. *New England Journal of Medicine*, 360 (11), 1085-1095.

Jiang, B., Liang, S., Peng, Z., Cong, H., Levy, M., Cheng, Q., Wang, T., Remais, J.V. 2017. Transport and public health in China: the road to a healthy future. *The Lancet,* 390, 1781-1791.

Kam, W., Liacos, J., Schauer, J., Delfino, R., Sioutas, C. 2012. Size-segregated composition of particulate matter (PM) in major roadways and surface streets. *Atmospheric environment,* 55, 90-97.

Krecl, P., Harrison, R.M., Johansson, C., Targino, A. C., Beddows, D.C., Ellermann, T., Ketzel, M. 2021. Long-term trends in nitrogen oxides concentrations and on-road vehicle emission factors in Copenhagen, London and Stockholm. *Environmental Pollution*, 290, 118105.

Kunzli, N., Kaiser, R., Medina, S., Studnicka, M., Chanel, O., Filliger, P., Herry, M., Horak JR, F., Puybonnieux-Texier, V., Quenel, P. 2000. Public-health impact of outdoor and traffic-related air pollution: a European assessment. *The Lancet,* 356, 795-801.

Lei, T., Zhang, W., Lin, Z., Zhang, H., Xi, Z., Chen, J., Wei, W. 2012. Impact of traffic emissions on local air quality and the potential toxicity of traffic-related particulates in Beijing, China. *Biomedical and Environmental Sciences,* 25(6), 663-671.

Li, B., Ho, S., Xue, Y., Huang, Y., Wang, L., Cheng, Y., Dai, W., Zhong, H., Cao, J., Lee, S. 2017. Characterizations of volatile organic compounds (VOCs) from vehicular emissions at roadside environment: The first comprehensive study in Northwestern China. *Atmospheric Environment,* 161, 1-12.

Liu, Q., Liu, Y., Yin, J., Zhang, M., Zhang, T. 2014. Chemical characteristics and source apportionment of $PM_{10}$ during Asian dust storm and non-dust storm days in Beijing. *Atmospheric Environment,* 91, 85-94.

Ma, C. J., & Kang, G. U. 2020. Air quality variation in Wuhan, Daegu, and Tokyo during the explosive outbreak of COVID-19 and its health effects. *International Journal of Environmental Research and Public Health*, 17(11), 4119.

MEIC 2018. Multi-resolution Emission Inventory in China. Availabe on:
*http://www.meicmodel.org/dataset-mix.html (updated to 30/08/2018)*.

National Health Commission of the People's Republic of China, 2015. China Health Statistics Yearbook 2014. *Peking Union Medical College Press*, Beijing, China.

National Health Commission of the People's Republic of China, 2021. China Health Statistics Yearbook 2020. *Peking Union Medical College Press*, Beijing, China.

Pant, P., Harrison, R.M. 2013. Estimation of the contribution of road traffic emissions to particulate matter concentrations from field measurements: a review. *Atmospheric environment,* 77, 78-97.

Rissler, J., Swietlicki, E., Bengtsson, A., Boman, C., Pagels, J., Sandstrom, T., Blomberg, A., Londahl, J. 2012. Experimental determination of deposition of diesel exhaust particles in the human respiratory tract. *Journal of Aerosol Science,* 48, 18-33.

Shi, Z., Song, C., Liu, B., Lu, G., Xu, J., VU, T.V., Elliott, R.J.R., Li, W., Bloss, W.J., Harrison, R.M. 2021. Abrupt but smaller than expected changes in surface air quality attributable to COVID-19 lockdowns. *Science Advances,* 7, eabd6696.

Srivastava, D., Xu, J., Vu, T.V., Liu, D., Li, L., Fu, P., Hou, S., Shi, Z., Harrison, R.M. 2021. Insight into $PM_{2.5}$ Sources by Applying Positive Matrix Factorization (PMF) at an Urban and Rural Site of Beijing. *Atmospheric Chemistry and Physics Discussions*, 1-51.

THORPE, A. & HARRISON, R. M. 2008. Sources and properties of non-exhaust particulate matter from road traffic: a review. *Science of the total environment,* 400, 270-282.

Sun, L., Zhang, T., Liu, S., Wang, K., Rogers, T., Yao, L., & Zhao, P. 2021. Reducing energy consumption and pollution in the urban transportation sector: A review of policies and regulations in Beijing. *Journal of Cleaner Production*, 285, 125339.

Turner, M. C., Jerrett, M., Pope III, C. A., Krewski, D., Gapstur, S. M., Diver, W. R., & Burnett, R. T. 2016. Long-term ozone exposure and mortality in a large prospective study. *American journal of respiratory and critical care medicine*, 193 (10), 1134-1142.

Tong, R., Liu, J., Wang, W., Fang, Y. 2020. Health effects of $PM_{2.5}$ emissions from on-road vehicles during weekdays and weekends in Beijing, China. *Atmospheric Environment,* 223, 117258.

Vu, T.V., Shi, Z., Cheng, J., Zhang, Q., He, K., Wang, S., Harrison, R.M. 2019. Assessing the impact of clean air action on air quality trends in Beijing using a machine learning technique. *Atmospheric Chemistry and Physics,* 19, 11303-11314.

Vu, T.V., Zauli-Sajani, S., Poluzzi, V., Harrison, R.M. 2018. Factors controlling the lung dose of road traffic-generated sub-micrometre aerosols from outdoor to indoor environments. *Air Quality, Atmosphere & Health,* 11, 615-625.

Wang, F., Ketzel, M., Ellermann, T., Aring, Hlin, P., Jensen, S. S., Fang, D., Massling, A. 2010. Particle number, particle mass and $NO_x$ emission factors at a highway and an urban street in Copenhagen. *Atmospheric Chemistry and Physics.,* 10, 2745-2764.

Wu, S., Deng, F., Wei, H., Huang, J., Wang, X., Hao, Y., Zheng, C., Qin, Y., Lv, H., Shima, M. 2014. Association of cardiopulmonary health effects with source-appointed ambient fine particulate in Beijing, China: a combined analysis from the Healthy Volunteer Natural Relocation (HVNR) study. *Environmental science & technology,* 48, 3438-3448.

Xu, J., Srivastava, D., Wu, X., Hou, S., Vu, T.V., Liu, D., Sun, Y., Vlachou, A., Moschos, V., Salazar, G. 2021. An evaluation of source apportionment of fine OC and $PM_{2.5}$ by multiple methods: APHH-Beijing campaigns as a case study. *Faraday Discussions,* 226, 290-313.

Xu, X., Zhang, T. 2020. Spatial-temporal variability of $PM_{2.5}$ air quality in Beijing, China during 2013–2018. *Journal of environmental management,* 262, 110263.

Xue, L., Wang, T., Louie, P., Luk, C., Biake, D. R., & Zheng, X. 2014. Increasing external effects negate local efforts to control ozone air pollution: a case study of hong kong and implications for other chinese cities. *Environmental Science & Technology*, 48 (18), 10769-10775.

Yang, X., Liang, F., Li, J., Chen, J., Liu, F., Huang, K., Cao, J., Chen, S., Xiao, Q., Liu, X. 2020. Associations of long-term exposure to ambient $PM_{2.5}$ with mortality in Chinese adults: A pooled analysis of cohorts in the China-PAR project. *Environment international,* 138, 105589.

Yang, Z., Wang, H., Shao, Z., Muncrief, R. 2015. Review of Beijing's comprehensive motor vehicle emission control programs. *communications,* 49, 847129-102.

Yi, S. J., Shon, C., Min, K. D., Kim, H. C., Leem, J. H., Kwon, H. J., & Kim, S. Y. 2017. Association between exposure to traffic-related air pollution and prevalence of allergic diseases in children, Seoul, Korea. *BioMed research international*, 2017.

Yin, P., Brauer, M., Cohen, A., Burnett, R.T., Liu, J., Liu, Y., Liang, R., Wang, W., Qi, J., Wang, L. 2017. Long-term fine particulate matter exposure and nonaccidental and cause-specific mortality in a large national cohort of Chinese men. *Environmental health perspectives,* 125, 117002.

Zhang, Q., Zheng, Y., Tong, D., Shao, M., Wang, S., Zhang, Y., Xu, X., Wang, J., He, H., Liu, W., Ding, Y., Lei, Y., Li, J., Wang, Z., Zhang, X., Wang, Y., Cheng, J., Liu, Y., Shi, Q., Yan, L., Geng, G., Hong, C., Li, M., Liu, F., Zheng, B., Cao, J., Ding, A., Gao, J., Fu, Q., Huo, J., Liu, B., Liu, Z., Yang, F., He, K., Hao, J. 2019a. Drivers of improved $PM_{2.5}$ air quality in China from 2013 to 2017. *Proceedings of the National Academy of Sciences,* 116, 24463-24469.

Zhang, S., Wu, Y., Yan, H., Du, X., Zhang, K. M., Zheng, X., Fu, L., Hao, J. 2019b. Black carbon pollution for a major road in Beijing: Implications for policy interventions of the heavy-duty truck fleet. *Transportation Research Part D: Transport and Environment,* 68, 110-121.

Zhong, J., Zhang, X., Wang, Y., Sun, J., Zhang, Y., Wang, J., Tan, K., Shen, X., Che, H., Zhang, L. 2017. Relative contributions of boundary-layer meteorological factors to the explosive growth of $PM_{2.5}$ during the red-alert heavy pollution episodes in Beijing in December 2016. *Journal of Meteorological Research,* 31, 809-819.